L-band PS analysis: JERS-1 results and TerraSAR–L predictions

Kenji Daito[1], Alessandro Ferretti[2], Shigeki Kuzuoka[3],Fabrizio Novali[2], Pietro Panzeri [2], Fabio Rocca [4]

[1] Daido Institute of Technology, 10-3 Takiharu-cho, Minami-ku, Nagoya
[2] TRE, Via Vittoria Colonna 7, Milano, Italy
[3] ImageONE,Shinjuku Daiichiseimei Bldg. 12F 2-7-1, Nishi Shinjuku, Shinjuku Tokyo 163-0712 Japan
[4]Politecnico di Milano, Piazza Leonardo da Vinci 32 Milano, Italy

Abstract
Long term interferometry with L band can be studied using data from the Japanese satellite JERS, that flew from 1992 to 1998. Notwithstanding problems like electromagnetic interference and limited information on the across track baselines, still the quality of the system makes the data very useful. This makes it possible the identification of Permanent Scatterers in urban and semi urban areas, with very high density (up to 150/km^2) with coherence up to .9 in an interval of time of several years. In turn, this allows the better determination of the orbits, and allows a comparison with similar data from ERS 1. Namely, a similarity is found with data acquired during the 3 days repeat cycle. The longer wavelength therefore is seen to correspond to a longer decay time of the temporal coherence, thus explaining the high quality results obtained. The higher average coherence allows to combine the phase information of several adjacent points, and therefore to at least partially reduce the effects of the higher geometric dispersion of the differential interferometry outcomes due to the very same longer wavelength. In conclusion, while the technique appears too coarse for direct estimation of building motion, it appears very interesting for vegetated areas and for areas where the velocity of the motion would create alias in C band.

Introduction
The Japanese satellite JERS-1 has been operational from 1992 to 1998. It used a sensor in L band (λ=23,5cm, f_0=1.275GHz, 18x6m ground range x azimuth resolution) with polarization HH; it had a sun-synchronous orbit with altitude 568 km. Images were acquired every 44 days. The acquisition angle is 35°, greater than ERS-1, and the foreshortening effect is weaker. Moreover, the orbit is lower and allows getting a resolution higher than in case of ERS. The longer wavelength makes JERS useful for geologic applications in areas covered by vegetation, due to the higher penetration of the signal.
Unfortunately, JERS images are affected by various problems (ambiguity in azimuth values, imprecision of the on board clock, low signal to noise ratio, limited information from ephemeredes, etc.) caused by a power loss of the signal transmitted from the platform to the ground. Images are also more sensible to noise due to the interaction with ground radars.

Figure 1: C band and L band (SIR-C/X-SAR images of Flevoland in Holland).
color scheme: HH: red, HV:green, VV: blue

ERS satellites operate in C band with VV polarization, while JERS uses L band with HH polarization. Both ERS and JERS show a strong layover effect. Due to its acquisition geometry, ERS is twice as sensible to the vertical component of displacement as JERS. Figure 2 allows a comparison of the geometric distortions of the two sensors.

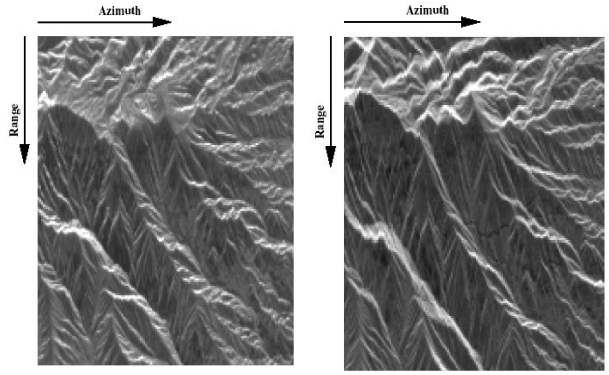

Figure 2: Reflectivity images of ERS-1 and JERS-1 over an area in Japan near Fuji City.

.

Interferometry in C and L bands

One of the main applications of SAR techniques is interferometry. C band has a wavelength which is ¼ of the wavelength of L band and we can detect variations of height with a resolution 4 times higher. For JERS the critical value of the baseline is 5.7 km; for ERS is 1.1 km. The following figure represents two interferograms of the same area created with the two sensors in a similar time interval on Fuji City area: the coherence on urban areas is about the same; on vegetated areas, there is no competition.

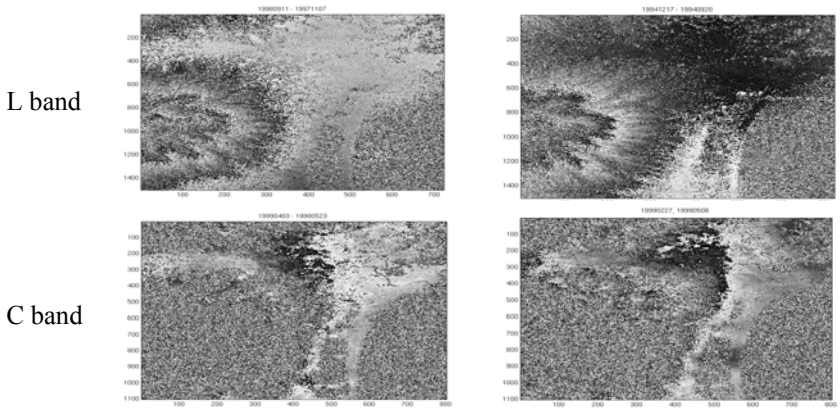

Figure 3: Interferograms with similar altitude of ambiguity in L band and C band .

State vectors inaccuracies and radio frequency interference (RFI)

We now describe the difficulties encountered during JERS-1 data processing and the solutions adopted. JERS data suffer from two problems: state vectors inaccuracies and radio frequency interference (RFI) [1]. The images have been processed with an orbital information correction algorithm, through which it was possible to retrieve a set of optimised baselines. The baseline correction shows a strong correlation with the acquisition time: such a dependency is probably caused by a satellite drift, which is in general difficult to estimate and correct; in this case the error at a first analysis seems to follow a linear dependency, as it can be seen in figure 4, which reports the drift in meters with respect to the orbit supplied by NASDA. In DInSAR analysis, orbit inaccuracies create low order polynomial phase components on

the differential interferograms plus phase artefacts proportional to the local topography. This second term is usually negligible in ERS. On the contrary, they cannot be considered "second order effects" in JERS. In general, even in conventional DInSAR analysis, phase planes are systematically removed from differential interferograms, without re-estimating the orbits. We optimised the normal baseline for all the images used in the processing. The results turned out to be satisfactory. The basic idea is very easy: from an estimation of the low-order polynomial phase components, new baseline values are estimated and new differential interferograms are generated. This is obtained by exploiting all the available information and also estimating a second order polynomial to fit the trend in the drift.

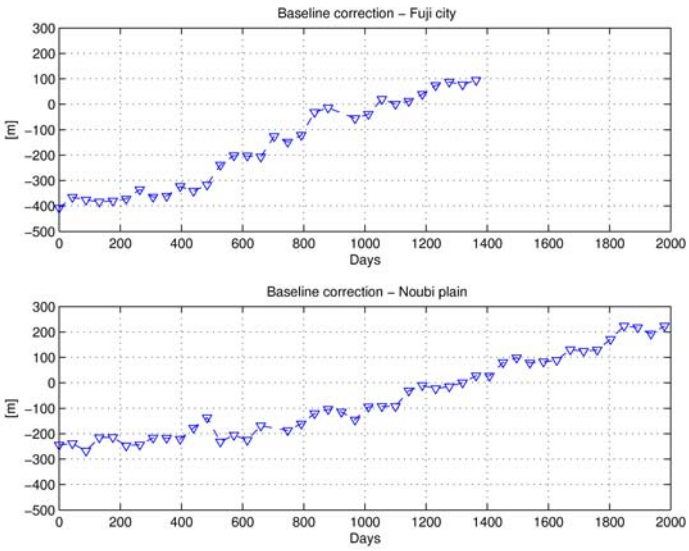

Figure 4:. Baselines corrections for images in the Fuji area (top) and Noubi plane (down).

Once the orbital errors are removed, interferograms quality shows a significant improvement if compared to original ones.

Radio frequency interference (RFI) improvement

During the processing of JERS data it became clear that the lower quality, if compared with ERS and Radarsat counterparts, is also due to noise superposed to the signal. This is sometimes so strong to be clearly visible on the focused image. Figure 5 shows the power spectrum of the data and a spike due to an interfering tone is visible. In Figure 6 a comparison is shown before and after the interference filtering. The quality improvement is visible.

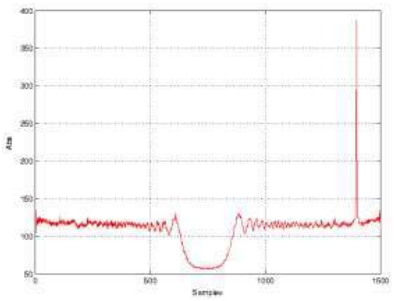

Figure 5: Spectrum of radio frequency signal: the spike due to an interfering tone is visible;

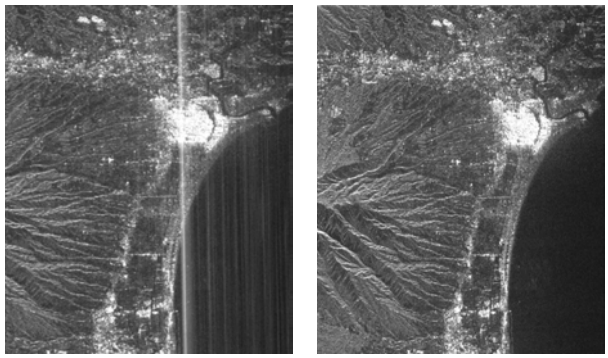

Figure 6: Fuji City images before and after interference noise removal.

Notch filter

The method adopted was the application of a zero-phase notch filter on the raw data before range compression on a line-by-line basis. A deeper analysis of the interference revealed that the frequency of the interference is not constant along the azimuth direction and produces signal peaks over small and well limited areas. This lead to an improvement of the notch filter. Beyond the higher visual quality of the image, the radio frequency interference removal resulted in noticeable improvements of the Doppler centroid estimate.

$\gamma > 0.7$ $\gamma > 0.9$

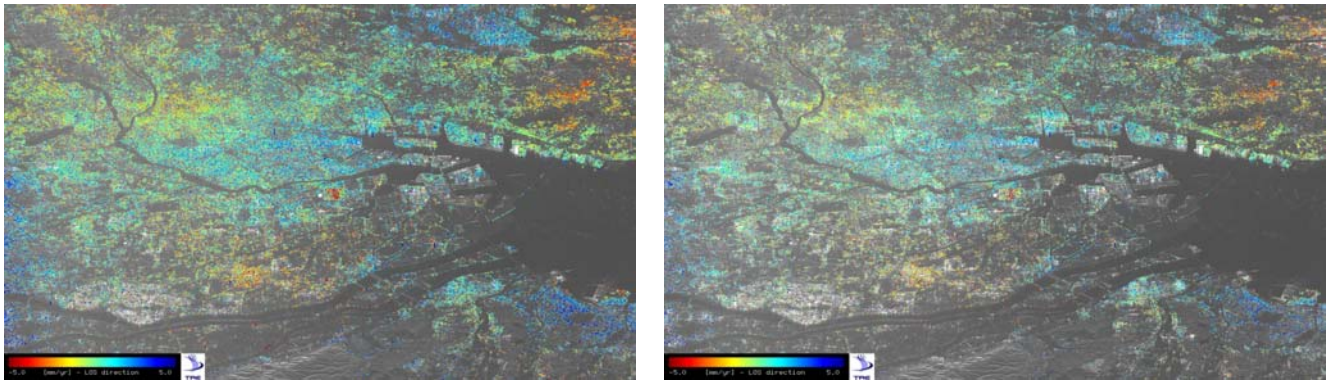

Figure 7: Permanent scatterers in the Noubi plane: left: γ>.7; 760000PS; right γ>.9; 240000PS

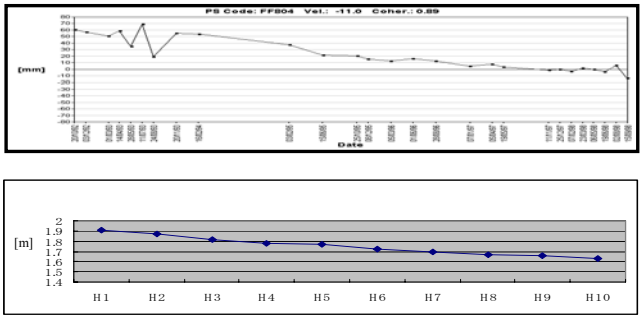

Figure 8: Selected PS ground motion and ground truth (H1 to H10 = 1989 to 1998).

Permanent Scatterers in L band in the Noubi area.

The Permanent Scatterers (PS) Technique is an interferometric technique developed at the Politecnico di Milano, through which it is possible to detect stable objects and measure their motion with high precision (down to few millimetres per year) [2, 3, 4]. The microwave signal reflected back to the sensor changes due to atmospheric conditions, terrain moisture, DC and baseline variations, etc. The PS algorithm allows removing these changes and isolating differences due to the object motion only. It is applicable to objects having a very high and stable signal reflectivity and with limited size, to remove variations of the reflectivity with the Line of Sight direction. Typically, these objects are parts of artificial structures like bridges, facades or building corners or rock outcrops. These objects are called Permanent Scatterers or PS. The output of the PS technique is a set of points whose average motion along LOS is given in millimetres per year. A PSInSAR analysis was carried out by TRE on the Noubi plain area. In Figure 7 the distribution of the PS in the area (approximately 2000 km^2) is shown, having coherence greater than .7 and .9 respectively. The high density of PS with a very high coherence shows that the image focus, satellite orbit determination and interference suppression have been successful. As a further proof of the quality of the results, a comparison of the motion of a selected PS with the locally available ground truth is provided in figure 8. The check is quite satisfactory. However, the level of the residuals measured in mm is quite noticeable with respect to that usual for C band. In fact, if we call σ_φ the phase dispersion, σ_x the motion dispersion, the latter changes with the ratio of the wavelengths. Then, if we suppose to have identical motion dispersion σ_x at all bands, we get the formula shown in the following. This formula is **underestimating** the coherence at longer wavelengths, since it neglects the greater

penetration and thus the probable lower motion dispersion. **Still, the coherence scales with the power of the wavelengths ratio, squared**. The coherence in L band γ_L correspondent to the same motion dispersion as the one seen in C band is the $1/4^2$=1/16 power of γ_C. Thus, to γ_C =0.7 → γ_L =0.98; to γ_L =0.9 → γ_C =0.18. Again, this is a conservative estimate, since we are neglecting vegetation penetration that will further increase coherence at lower frequencies. By the same token, we can say that γ_L will be mostly limited by SNR, rather than by temporal decorrelation. In fact, hypothesizing an L band SNR equal to 20 dB and thus γ_L< 0.99 the equivalent γ_C would be < 0.85.

$$\gamma = e^{-\sigma_\varphi{}^2/2}; \quad \sigma_{x;C,L} = \frac{\lambda_{C,L}}{4\pi}\sigma_\varphi \rightarrow \gamma_C = \gamma_L^{\left(\frac{\lambda_L}{\lambda_C}\right)^2}$$

Discussion

In figure 9, we show the histogram of the amplitudes of the scatterers in L band, 44 days repeat, together with that of the PS. It is visible that PS have a higher amplitude than average, as rather obvious, but by and large, are a constant and high percentage of all the scatterers, above a minimum amplitude.

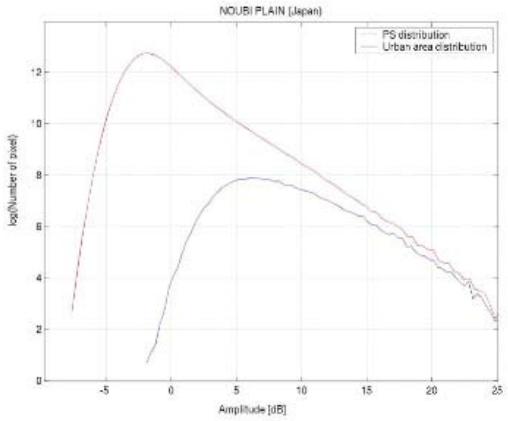

Figure 9: Histograms of amplitudes in an urban area and PS amplitudes: most high amplitude scatterers are PS

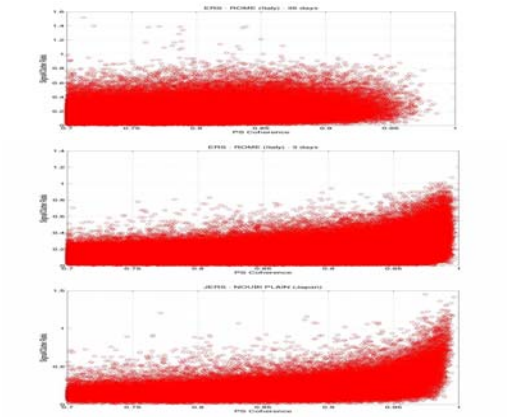

Figure 10: Cross plots of amplitudes versus coherence for C band 35 days repeat, C band 3 days, L band 44 days.

In Figure 10 we show the histograms of the distributions of the amplitudes of the PS versus their coherence, in three cases, namely C band 35 days repeat, C band, 3 days repeat, L band, 44 days repeat. While in C35 it is possible to have high amplitude scatterers with rather low coherence (the histogram is "fat" along the vertical direction) in C3 and L44 bands the histograms are "lean", in that practically all high amplitude scatterers show high coherence. In other words, it

appears that the longer the wavelength, the longer the decorrelation time, as mechanically reasonable. That the decorrelation time scales with the time squared and therefore with the wavelength inverse squared should be further researched; however, it could well explain the high quality of L band data and their similarity with C3 band data.

TerraSAR - L predictions

The changes from JERS to TerraSAR – L will be significant: better orbits, better SNR, smaller resolution cell by a factor greater than 5. This will immediately reflect on the quality of the PS interferometry. The PS can be expected practically everywhere, so that the atmospheric phase screen removal will be easy in vegetated areas too. The expected coherence might skyrocket to $0.7^{0.0625}=.98$ if the same mechanical stability of the objects in C band is expected. Obviously, many more objects will become visible, since coherence 0.7 in L band corresponds to coherence in C band equal to $0.7^{16}=0.003$ and areas where the coherence is now totally negligible, will be interferometrically visible.

Two points need further appreciation:

- the longer wavelength, besides making possible interferograms on vegetated areas, will be more robust with respect to motion with higher velocity, as expected in land sliding areas. There, motion of several centimeters per year or more should be expected; this kind of motion is likely to be aliased in C band, not to speak about X band. It will be quite visible in L band.
- the higher coherence will yield more points selectable as PS. Even if the precision of the single measurement may be low (since it scales with the wavelength), the favorable statistics will allow the increment of the precision by averaging.

Finally, the penetration in the vegetation, will allow the study of the ground reflections in highly vegetated areas and therefore studies of the biomass, Digital Elevation Models in forests, etc.

Conclusions

This analysis of the data set taken by JERS in the Noubi area has allowed, after the corrections made to improve the orbit estimates and to remove radio frequency interference, the determination of a very high number of Permanent Scatterers. The results are consistent with the theoretical hypothesis of high coherence in L band, namely that:

$$\gamma_L = \gamma_C^{\left(\frac{\lambda_C}{\lambda_L}\right)^2}$$

In turn, this allows to predict a very high interferometrical quality for L band imagery. Furthermore, the increased penetration in the vegetation, and the optimal predictable signal to noise ratio will make the TerraSAR – L very useful for centimetric measurements of ground motion in vegetated, volcanic, land sliding areas. TerraSAR – L will thus be an extremely important complement to C band data, this one to be used for millimetric measurements of subsidence and building motion.

References

[1] L. Giordani, P. Panzeri; *Elaborazioni di immagini JERS per applicazioni interferometriche;* Tesi di laurea in Ingegneria delle Telecomunicazioni, Politecnico di Milano, 20-02-2003.

[2] A. Ferretti, C. Prati, F. Rocca; *Nonlinear subsidence rate estimation using permanent scatterers in differential SAR interferometry.* IEEE Trans. Geosci. Remote Sensing, vol.38, pp. 2202-2212, Sept. 2000.

[3] A. Ferretti, C. Prati, F. Rocca; *Permanent scatterers in SAR interferometry.* IEEE Trans. Geosci. Remote Sensing, vol.39, pp. 8-20, Jan. 2001.

[4] C. Colesanti, A. Ferretti, F. Novali, C. Prati, F. Rocca; *SAR Monitoring of Progressive and Seasonal Ground Deformation Using the Permanent Scatterers Technique.* IEEE Trans. Geosci. Remote Sensing, Vol.41, No. 7, July 2003.